

### Pressure dependence of 4*f* levels in europium pentaphosphate up to 400 kbar

G. Huber,\* K. Syassen,<sup>†</sup> and W. B. Holzapfel

Max-Planck-Institut für Festkörperforschung, 7 Stuttgart 80, Federal Republic of Germany

(Received 14 February 1977)

The effect of pressure on the fluorescence of Eu<sup>3+</sup> ions in Europium pentaphosphate (EuP<sub>5</sub>O<sub>14</sub>) was measured up to 400 kbar. We observed a pressure induced “antilevel crossing” of the crystal-field levels within the <sup>7</sup>F<sub>1</sub> manifold and a decrease of the spin-orbit and Coulomb interactions for the 4*f* electrons, which is correlated with an expansion of the 4*f*-electron wave functions.

#### I. INTRODUCTION

The effect of pressure on the fluorescence of rare-earth ions in a crystalline environment is determined by different contributions like electronic shielding, hybridization of 4*f* wave functions, strength, and symmetry of the crystal field. The pressure-dependent variation of the balance between these interactions yields three different shifts:

- (a) The shift of the centers of gravity of the *LS* manifolds with respect to each other due to variations in the Coulomb interaction.
- (b) The shift of the center of gravity of each crystal-field-split *J* manifold (for a given *LS* value) which results from variations of the spin-orbit-coupling constant  $\xi_{4f}$ .
- (c) The shift of the Stark levels (of one *LSJ* manifold) with respect to each other due to variations of the crystal field in strength and symmetry. In first approximation, one would expect the following shift of Stark levels under pressure: Consider transitions between states  $|L, S, J\rangle$ , which are split in a given crystal field as shown in Fig. 1. In a first approximation, assuming a point-charge model, the crystal field increases with pressure. Therefore the energy separation of the states increases. The rate of increase depends thereby on the nature of the matrix elements between the states. Owing to the spread out of the individual states, luminescence lines may shift to higher as well as lower energies. This pressure dependence has been found in fact by Keating and Drickamer<sup>1</sup> for several rare-earth compounds.

However, preliminary high-pressure studies of the fluorescence of europium pentaphosphate (EuP<sub>5</sub>O<sub>14</sub>) up to<sup>2</sup> 50 kbar, indicated that the splitting of the Stark levels does not show a simple increase in this case. An extrapolation of the results suggested a possible phase transition at about 150 kbar. Recent developments of the high-pressure techniques for optical studies enabled us to extend these measurements up to and beyond

this pressure.

The optical and crystallographic properties of EuP<sub>5</sub>O<sub>14</sub> at normal pressure are summarized in Sec. II, then we describe the present technique for optical spectroscopy at high pressures. We present results on the pressure dependence of the fluorescence of EuP<sub>5</sub>O<sub>14</sub> up to 400 kbar. Finally, we describe the pressure dependence of the crystal-field splitting and the spin-orbit interaction for the Eu<sup>3+</sup> ions.

#### II. EUROPIUM PENTAPHOSPHATE

EuP<sub>5</sub>O<sub>14</sub> is a stoichiometric compound with a high concentration of active Eu<sup>3+</sup> ions ( $4 \times 10^{21}/$

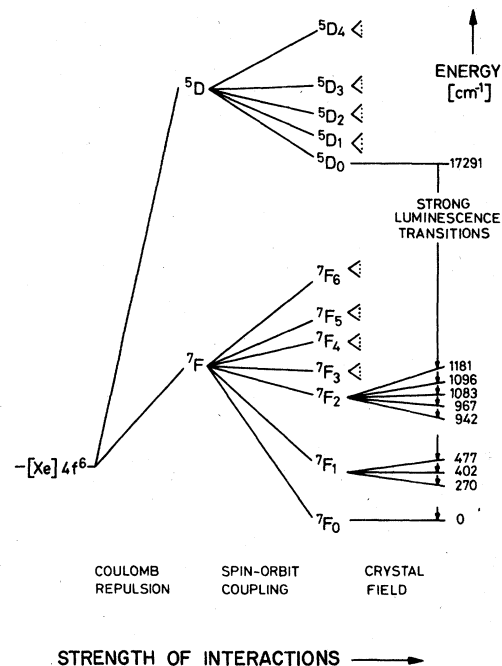


FIG. 1. Schematic representation of the energy levels of Eu<sup>3+</sup> showing the effects of Coulomb repulsion, spin-orbit coupling, and crystal-field interaction.

cm<sup>3</sup>). In this compound, all Eu<sup>3+</sup> ions occupy equivalent lattice sites. This is a major advantage for studying the pressure dependence of optical spectra, since there is the same change of the crystal field for all the active ions.

The crystal growing process, crystallography and indicatrix of EuP<sub>5</sub>O<sub>14</sub> is quite similar to the laser material NdP<sub>5</sub>O<sub>14</sub>.<sup>3-7</sup> The space group of the compound is *P2<sub>1</sub>/c*. The luminescence spectra of EuP<sub>5</sub>O<sub>14</sub> at atmospheric pressure are well known.<sup>7-9</sup> Figure 2 shows some of the <sup>5</sup>D<sub>0</sub> - <sup>7</sup>F luminescence at 4.2 and 300 K. The transition <sup>5</sup>D<sub>0</sub> - <sup>7</sup>F<sub>1</sub> is of magnetic dipole character, whereas the <sup>5</sup>D<sub>0</sub> - <sup>7</sup>F<sub>0</sub> and <sup>5</sup>D<sub>0</sub> - <sup>7</sup>F<sub>2</sub> transitions are electric dipole transitions.<sup>8</sup> The analysis of polarized spectra yields an effective site symmetry C<sub>s</sub> for the active Eu<sup>3+</sup> ion in the pentaphosphate lattice.<sup>8,9</sup>

### III. EXPERIMENTAL TECHNIQUE

The pressure for the optical fluorescence measurements is generated by a diamond anvil device.<sup>10</sup> The insert in Fig. 3 gives a schematic drawing of the inner parts of the device, which follows a design described by Barnett, Block, and Piermarini.<sup>11</sup> The pressure is generated by forcing two diamond anvils together, thereby deforming a metal gasket. The flats of the diamonds have octagonal shape with about 0.8 mm across. The diamonds are sintered into bronze. The hole in the gasket represents the actual pressurized chamber, containing the sample, a pressure sensor, and a

pressure-transmitting medium. A tilting and translational diamond mount allow for precise adjustments of the two diamond anvils with respect to each other. The device produces forces up to 30 kN to generate pressures in the range 0-400 kbar.

Figure 3 shows a cutaway drawing of the present diamond anvil cell. The force between the diamond anvils is generated by a lever mechanism.<sup>12</sup> By turning two coupled threads, the lower end points of the lever arm are moved towards each other. Thereby the distance between the upper end points of the lever arms decreases and the moving piston is pushed into the cell body. The long guidance of the moving piston assures parallelism of the diamond faces at high load.

In the present experiment we used either H<sub>2</sub>O or a 4:1 mixture of methanol and ethanol as pressure transmitting medium. Methanol-ethanol assures a truly hydrostatic pressure up to about 100 kbar.<sup>13</sup> Above 100 kbar pressures are "quasi-hydrostatic."

The pressure in the sample chamber was determined by the ruby fluorescence method,<sup>11</sup> taking the linear pressure dependence of the ruby *R* lines shift<sup>14</sup>  $dv/dP = -0.753 \text{ cm}^{-1}/\text{kbar}$  in the entire pressure range.

The optical fluorescence measurements were performed by exciting the sample and detecting the fluorescence through one of the diamond anvils as schematically indicated in Fig. 3. The sample was excited either by one of the argon laser lines or by directly pumping into the <sup>5</sup>D<sub>0</sub> level of EuP<sub>5</sub>O<sub>14</sub> using a tunable dye laser. The fluorescence radiation was passed through a 0.75-m spectrometer (Spex doublemate) and recorded with a standard photon counting system.

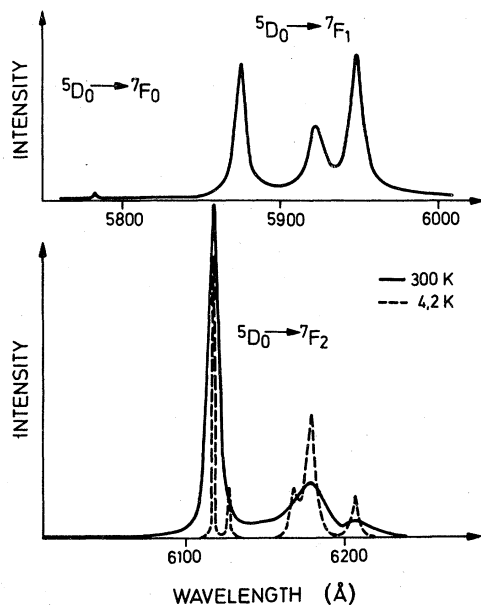


FIG. 2. Luminescence spectra of EuP<sub>5</sub>O<sub>14</sub> at 1 bar at 4.2 and 300 K.

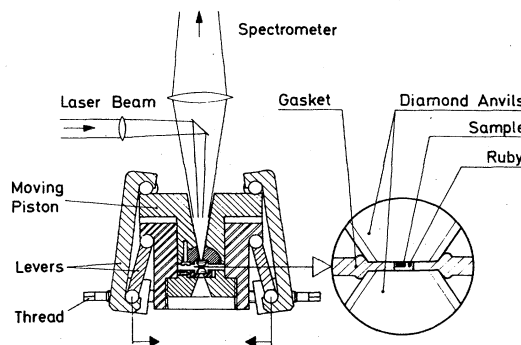


FIG. 3. Cross-section drawing of the diamond-anvil high-pressure cell showing the optical path, the force-generating device, and an enlarged view of gasket and sample. Typical dimensions of the sample chamber are 0.2 mm diameter and 0.1 mm thickness.

## IV. EXPERIMENTAL RESULTS

The fluorescence spectra  ${}^5D_0 \rightarrow {}^7F_0$ ,  ${}^7F_1$ ,  ${}^7F_2$  have been recorded at room temperature and various pressures between 0 and 400 kbar. Typical spectra for the transition  ${}^5D_0 \rightarrow {}^7F_1$  are shown in Fig. 4 for three different pressures. One may notice a shift of the center of gravity of the  ${}^5D_0 \rightarrow {}^7F_1$  transition as well as changes in the splitting of the  ${}^7F_1$  manifold. The effect of pressure on the energies of the  ${}^5D_0$ ,  ${}^7F_1$ , and  ${}^7F_2$  manifolds is represented in Figs. 5 and 6, where all the energies are given with respect to the ground state  ${}^7F_0$ . The broken lines illustrate the variations in the centers of gravity (CG). Strong nonlinear shifts are observed at the higher pressures.

With increasing pressure, the total splitting of the  ${}^7F_1$  manifold (Fig. 5) decreases at first. The separation between the lower two levels approaches a minimum separation of about  $30 \text{ cm}^{-1}$  at 150 kbar. Furthermore, a similar behavior is found at about 320 kbar for the upper two levels.

The variation of the  ${}^7F_2$  Stark levels (Fig. 6) shows the normal behavior under pressure. The total splitting of the  ${}^7F_2$  manifold increases under pressure. Pressure coefficients of the individual Stark levels range from  $-0.7$  to  $+0.5 \text{ cm}^{-1}/\text{kbar}$ .

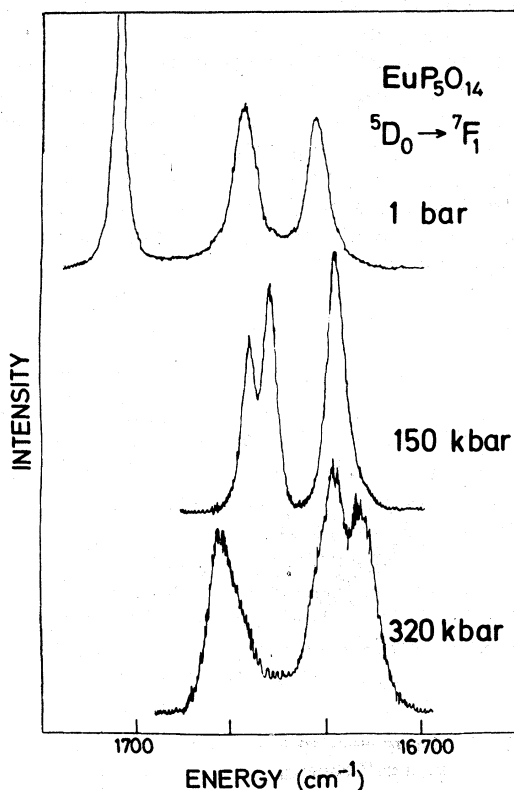


FIG. 4.  ${}^5D_0 \rightarrow {}^7F_1$  luminescence spectra of  $\text{EuP}_5\text{O}_{14}$  at room temperature and various pressures.

## V. DISCUSSION

In this chapter, we will concentrate on the discussion of two aspects of the experimental result: (i) the anomalous dependence of the Stark splitting for the  ${}^7F_1$  states; and (ii) the variation of the centers of gravity, i.e., the pressure dependence of the Coulomb and the spin-orbit interaction.

## A. Stark splitting

Since all the Stark levels of the  ${}^7F_1$  and the  ${}^7F_2$  manifold remain undegenerate, the site symmetry must be either triclinic, monoclinic or orthorhombic (see Table I) or without any symmetry. Measurements of polarized spectra at  $8.9$  bar are compatible only with an effective site symmetry  $C_s$  or lower. If one assumes that the effective site symmetry is in fact  $C_s$ ,<sup>8,9</sup> the representation of the  ${}^7F_1$  level is given by

$$|{}^7F_1\rangle = \Gamma_1 + \Gamma_1 + \Gamma_2,$$

and the polarized spectra support an assignment

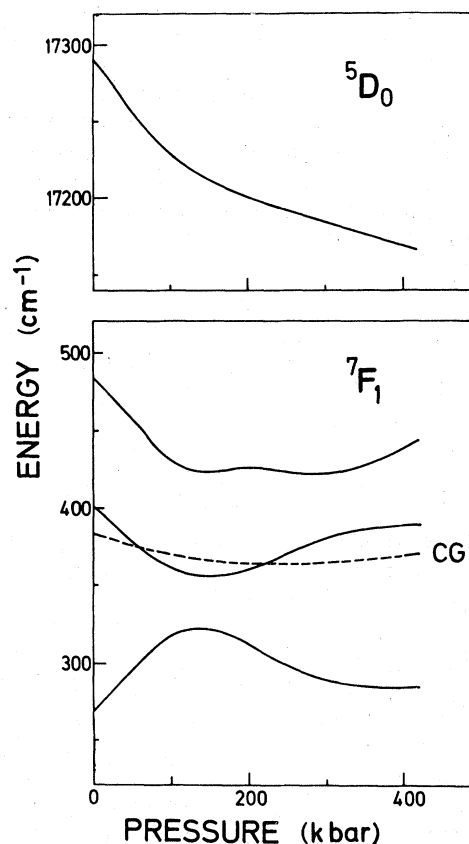


FIG. 5. Effect of pressure on the  ${}^5D_0$  and  ${}^7F_1$  energy levels of  $\text{Eu}^{3+}$  in  $\text{EuP}_5\text{O}_{14}$ . Energies are given with respect to the  ${}^7F_0$  ground state. Broken line represents the center of gravity (CG) and the  ${}^7F_1$  manifold.

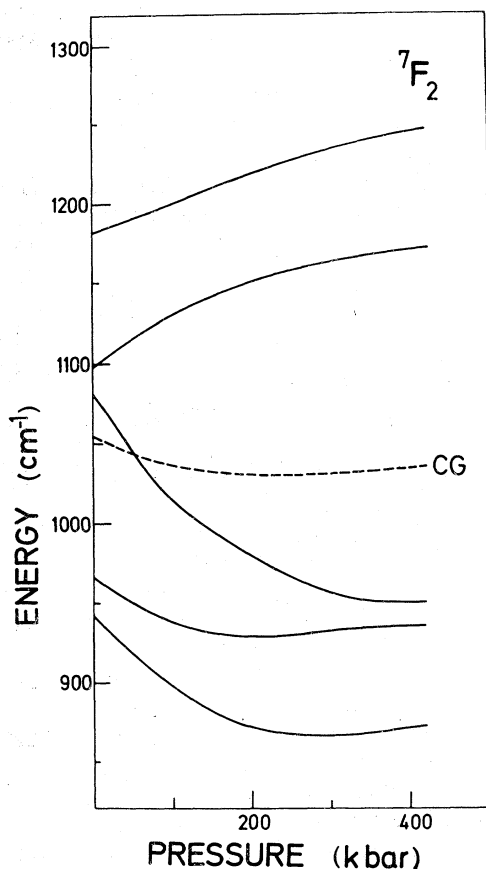


FIG. 6. Effect of pressure on the  ${}^7F_2$  energy levels of  $\text{Eu}^{3+}$  in  $\text{EuP}_5\text{O}_{14}$ . Broken line represents the center of gravity (CG).

of  $\Gamma_1$  character to the two lower levels of the  ${}^7F_1$  multiplet at 1 bar (Fig. 5), and of  $\Gamma_2$  to the upper level. The crystal field at the  $\text{Eu}^{3+}$  sites can be considered as having four components of different symmetry:

$$V = V_0 + V_{D_4} + V_{C_s} + V_n.$$

The cubic component  $V_0$  gives no splitting of the  ${}^7F_1$  multiplet. The tetragonal component  $V_{D_4}$  splits the  ${}^7F_1$  triplet into a singlet and a doublet and the

TABLE I. Number of Stark levels of  $\text{Eu}^{3+}$  for various site symmetries.

Site symmetry	Number of Stark levels		
	${}^7F_0$	${}^7F_1$	${}^7F_2$
Triclinic	1	3	5
monoclinic	1	2	4
orthorhombic	1	2	3
Tetragonal	1	1	2
Hexagonal rhombohedral	1	1	2
Cubic	1	1	2

component with  $C_s$  symmetry  $V_{C_s}$  as well as the component with no symmetry  $V_n$  remove the degeneracy completely. Therefore, the decrease of the splitting between the two lower ( $\Gamma_1$ ) levels of the  ${}^7F_1$  multiplet (Fig. 5) indicates an approach toward a tetragonal site symmetry in the pressure range from 0 to 100 kbar,<sup>2</sup> whereas the decrease of the splitting between the upper ( $\Gamma_2$ ) level and the center of gravity of the two lower ( $\Gamma_1$ ) levels reflects a decrease of the tetragonal crystal field component in this pressure range. If one extrapolates the low-pressure variation of these levels linearly to pressures in excess of 100 kbar, one would find at first a crossover of the two lower ( $\Gamma_1$ ) levels at about 150 kbar and a crossover of the upper ( $\Gamma_2$ ) level with the center of gravity of the two lower ( $\Gamma_1$ ) levels at about 300 kbar. The first crossover would correspond to a continuous variation of  $V_{C_s}$  through 0 whereas the second crossover reflects a similar variation for  $V_{D_4}$  at higher pressures. However, in contrast to this "linear extrapolation," the  ${}^7F_1$  multiplet remains nondegenerate in the whole pressure range up to 400 kbar (Fig. 5).

The antilevel crossing of the two lower ( $\Gamma_1$ ) levels can be explained by symmetry coupling<sup>15</sup> as well as by contributions from nonsymmetric crystal field component  $V_n$ . The antilevel crossing at about 300 kbar involves, on the other hand, levels of different representations in an effective  $C_s$  site symmetry and indicates, therefore, that the crystal-field component of no symmetry  $V_n$  contributes strongly to the splitting at high pressures. The assignment of dominant  $\Gamma_1$  and  $\Gamma_2$  character to the Stark levels of the  ${}^7F_1$  multiplet of  $\text{Eu}^{3+}$  in  $\text{EuP}_5\text{O}_{14}$  is therefore no longer meaningful at pressures in excess of 100 kbar and may be questionable even in the lower-pressure range.

#### B. Spin-orbit interaction and Coulomb interaction

In a first approximation, the center of gravity (CG) of each  ${}^7F_J$  manifold should be independent of the crystal field. On the other hand, the ligand orbitals affect the  $4f$  wave functions to give small variations of the spin-orbit coupling parameter  $\xi_{4f}$ . Under pressure one expects an increase in the overlap and, therefore, an increase in the splitting of the  $J$  manifolds with respect to each other. The variation of  $\xi_{4f}(P)$  can be determined from the present data by the use of the well-known Landé rule

$$E({}^7F_J) - E({}^7F_{J-1}) = (j/2S)\xi_{4f}.$$

The experimental values for the centers of gravity (CG) of the  $J = 1$  and 2 manifolds in Figs. 5 and 6 give a variation of the average value  $\xi_{4f}(P)/\xi_{4f}(0)$

shown in Fig. 7. The almost linear decrease of  $\xi_{4f}(P)$  up to about 100 kbar seems to slow down at higher pressures and may even turn over into an increase at pressures in excess of 300 kbar. Since it is well known<sup>16</sup> that the spin-orbit splitting is sensitive to uniaxial stresses, the minimum in Fig. 7 could be a result of anisotropic stresses at pressures in excess of 100 kbar. Therefore, only the initial slope  $d \ln \xi_{4f}/dP$  will be discussed in more detail.

Marshall and Stuart<sup>17</sup> have suggested that the effect of placing a free ion into a crystal leads to an expansion of the wave functions. This expansion is considered to result from the screening of the nuclear charge by the overlapping charge clouds from the ligands. In the present case, experimental evidence for this screening results from the decrease of the spin-orbit interaction.

Usually,<sup>17,18</sup> this effect of the ligands on the radial part of the wave functions of the central ion is described by a covalency factor  $\alpha^2$  or a scaling factor  $\beta = \alpha^{2/3}$  which expands the radial part of the 4f wave functions  $R_{4f}(r)$  with respect to the free-ion case,  $\beta = 1$ . If one assumes an effective Coulomb field on the active ion  $\text{Eu}^{3+}$ , the spin-orbit coupling should vary as

$$\langle r_{4f}^{-3} \rangle = \beta^3 \langle r_{4f}^{-3} \rangle_{\beta=1}$$

Within this model, we obtain from the initial slope in Fig. 7

$$\begin{aligned} E(^5D) - E(^7F) &= [E(^5D_0) - E(^7F_0)] - [E(^7F) - E(^7F_0)] + [E(^5D) - E(^5D_0)] \\ 52 F_2 \text{ (Ref. 19)} & \quad \text{see Fig. 5} \quad K_1 \xi_{4f}(^7F) \text{ (Ref. 8)} \quad K_2 \xi_{4f}(^5D) \text{ (Ref. 20)} \\ & \quad \sim 17\,300 \text{ cm}^{-1} \quad \sim 2536 \text{ cm}^{-1} \quad \sim 4700 \text{ cm}^{-1} \end{aligned}$$

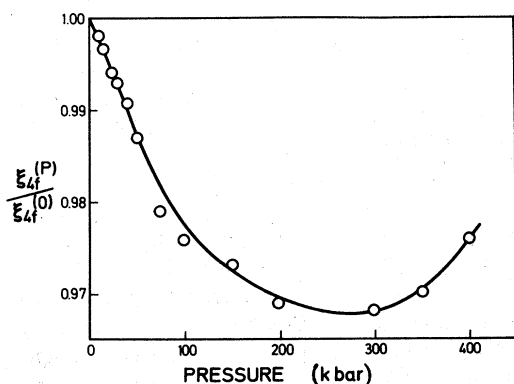


FIG. 7. Effect of pressure on the spin-orbit interaction  $\xi_{4f}(P)$  normalized to the 1-bar value  $\xi_{4f}(0)$  as estimated from the centers of gravity of the  $^7F_0$ ,  $^7F_1$ , and  $^7F_2$  manifolds.

$$\frac{d \ln \xi_{4f}}{dP} = \frac{d \ln \langle r_{4f}^{-3} \rangle}{dP} = -0.25 \text{ Mbar}^{-1}$$

and

$$\frac{d \ln \beta}{dP} = \frac{1}{3} \frac{d \ln \langle r_{4f}^{-3} \rangle}{dP} = -0.08 \text{ Mbar}^{-1}$$

If one uses a reasonable estimate for the volume compressibility of either the bulk material or the volume of the active ion, one finds that the volume dependence of  $\langle r_{4f}^{-3} \rangle$  in this compound is, as expected, about an order of magnitude smaller than the volume dependence of  $\langle r_{3d(t_2g)}^{-3} \rangle$  for the  $3d(t_2g)$  electron wave functions of, for instance,  $\text{Fe}^{2+}$  in  $\text{CoO}$ .<sup>18</sup>

On the other hand, we can estimate from the variation of the scaling parameter  $\beta$  the variation of the 4f electron Coulomb repulsion which should vary as  $\langle r_{4f}^{-1} \rangle$ . Within this scaling model, one obtains for the corresponding Slater integral

$$F_2 \sim \langle r_{4f}^{-1} \rangle = \beta \langle r_{4f}^{-1} \rangle_{\beta=1}$$

and for the pressure derivatives

$$\frac{d \ln F_2}{dP} = \frac{d \ln \beta}{dP} = -0.08 \text{ Mbar}^{-1}$$

This estimate can be compared with other experimental data. When one uses the present values for the variation of the energy difference  $E(^5D_0) - E(^7F_0)$  and of the variation of the average spin-orbit coupling parameter  $\xi_{4f}(^7F)$  of the  $^7F$  multiplet, and, furthermore, the assumption  $d \ln \xi_{4f}(^5D)/dP = d \ln \xi_{4f}(^7F)/dP$  and the relation

where  $E(^5D)$  and  $E(^7F)$  denote the centers of gravity of the total  $^5D$  and  $^7F$  manifolds, one obtains  $d \ln F_2/dP = -0.07 \text{ Mbar}^{-1}$ . This value is in good agreement with the value  $-0.08 \text{ Mbar}^{-1}$ , which was obtained from the pressure dependence of the spin-orbit coupling.

We have neglected so far some effects which may not only contribute to the initial pressure dependences but which may be furthermore involved in the change of the spin-orbit coupling under very high pressures (Fig. 7): (i) increasing gradient  $\partial V/\partial r$  of the effective potential, which should increase  $\xi_{4f}$ ; (ii) repulsion between 4f, 5s, 5p, orbitals of  $\text{Eu}^{3+}$  and 2s, 2p orbitals of  $\text{O}^{2-}$ ; (iii) increasing hybridization of 4f, 2s, and 2p orbitals<sup>17</sup>; (iv) decreasing overlap of the wave functions due to an angular distortion. It is obvious that all of

these effects may influence simultaneously the anti-level-crossing of the  ${}^7F_1$  levels and vice versa.

## VI. CONCLUSIONS

We have reported on a static high-pressure technique for optical studies at pressures up to 400 kbar. Owing to low-symmetry crystal-field components we observed a pressure-induced anti-level crossing of the  ${}^7F_1$  Stark levels in  $\text{EuP}_5\text{O}_{14}$  at 150 and 320 kbar. The variation of the spin-orbit interaction and Coulomb interaction is quantitatively explained by an expansion of the  $4f$  wave function. At 100 kbar a relative expansion of 0.8% decreases the Coulomb interaction by nearly the same amount, whereas the spin-orbit constant is

decreased by 2.5%. This is in agreement with the theory which gives  $H_{\text{Coulomb}} \sim \langle r^{-1} \rangle$  and  $H_{LS} \sim \langle r^{-3} \rangle$ . In the pressure range below 100 kbar the situation is quite clear, whereas at higher pressures either second-order effects or anisotropic stress contributions are dominant. Further measurements on stoichiometric rare earth compounds with higher symmetry may contribute even more detailed information about the different perturbations of the lanthanide ion.

## ACKNOWLEDGMENTS

We would like to thank Professor H. G. Danielmeyer for helpful discussions and comments. In addition we thank W. Dietrich, W. Böhringer, and E. Böttcher for excellent technical assistance.

\*Present address: Institut für Angewandte Physik, Universität Hamburg, 2000 Hamburg 36, Fed. Rep. of Germany.

† Present address: IBM Research Laboratory, 5600 Cottle Road, San Jose, Calif. 95193.

<sup>1</sup>K. B. Keating and H. G. Drickamer, *J. Chem. Phys.* **34**, 143 (1961).

<sup>2</sup>G. Huber, W. B. Holzapfel, and H. G. Danielmeyer, *Europhysics Conf. Abst.* **1**, 94 (1975).

<sup>3</sup>H. G. Danielmeyer and H. P. Weber, *IEEE J. Quantum Electron* **QE-8**, 805 (1972).

<sup>4</sup>H. P. Weber, T. C. Damen, H. G. Danielmeyer, and B. C. Tofield, *Appl. Phys. Lett.* **22**, 534 (1973).

<sup>5</sup>G. Huber, W. W. Krühler, W. Bludau, and H. G. Danielmeyer, *J. Appl. Phys.* **46**, 3580 (1975).

<sup>6</sup>H. G. Danielmeyer, J. P. Jeser, E. Schönherr, and W. Stetter, *J. Cryst. Growth* **22**, 298 (1974).

<sup>7</sup>G. Huber, J. P. Jeser, W. W. Krühler, and H. G. Danielmeyer, *IEEE J. Quantum Electron.* **QE-10**, 766 (1974).

<sup>8</sup>C. Brecher, *J. Chem. Phys.* **61**, 2297 (1974).

<sup>9</sup>G. Huber, Ph.D. thesis (Stuttgart, 1975) (unpublished).

<sup>10</sup>K. Syassen and W. B. Holzapfel (unpublished).

<sup>11</sup>J. D. Barnett, S. Block, and G. J. Piermarini, *Rev. Sci. Instrum.* **44**, 1 (1973).

<sup>12</sup>R. Keller and W. B. Holzapfel, *Rev. Sci. Instrum.* (to be published).

<sup>13</sup>G. J. Piermarini, S. Block, and J. D. Barnett, *J. Appl. Phys.* **44**, 5377 (1973).

<sup>14</sup>G. J. Piermarini, S. Block, J. D. Barnett, and R. A. Forman, *J. Appl. Phys.* **46**, 2774 (1975).

<sup>15</sup>H. Bethe, *Ann. Phys. (Leipz.)* **3**, 133 (1929).

<sup>16</sup>D. M. Adams, R. Appleby, and S. K. Sharma, *J. Phys. E* **9**, (1976).

<sup>17</sup>W. Marshall and R. Stuart, *Phys. Rev.* **123**, 2048 (1961).

<sup>18</sup>K. Syassen, and W. B. Holzapfel, *Phys. Rev. B* **8**, 1799 (1973).

<sup>19</sup>J. P. Elliott, B. R. Judd, and W. A. Runciman, *Proc. R. Soc. A* **240**, 509 (1957).

<sup>20</sup>G. H. Dieke, *Spectra and Energy Levels of Rare Earth Ions in Crystals* (Wiley, New York, 1969).